Journal of Quantitative Spectroscopy & Radiative Transfer 113 (2012) 1753–1761

Contents lists available at SciVerse ScienceDirect

Journal of Quantitative Spectroscopy & Radiative Transfer

journal homepage: www.elsevier.com/locate/jqsrt

Vertically constrained CO_2 retrievals from TCCON measurements

Le Kuai [a,*], Debra Wunch [a], Run-Lie Shia [a], Brian Connor [b], Charles Miller [c], Yuk Yung [a]

[a] Division of Geological and Planetary Sciences, California Institute of Technology, MC 150-21, Pasadena, CA 91125, USA
[b] BC Consulting Ltd., 6 Fairway Dr., Alexandra 9320, New Zealand
[c] Jet Propulsion Laboratory, California Institute of Technology, USA

ARTICLE INFO

Article history:
Received 28 October 2011
Received in revised form
24 April 2012
Accepted 26 April 2012
Available online 5 May 2012

Keywords:
TCCON
Carbon dioxide
Retrieval

ABSTRACT

Partial column-averaged carbon dioxide (CO_2) mixing ratio in three tropospheric layers has been retrieved from Total Carbon Column Observing Network (TCCON) spectra in the 1.6 μm CO_2 absorption band. Information analysis suggests that a measurement with ~60 absorption lines provides three or more pieces of independent information, depending on the signal-to-noise ratio and solar zenith angle. This has been confirmed by retrievals based on synthetic data. Realistic retrievals for both total and partial column-averaged CO_2 over Park Falls, Wisconsin on July 12, 15, and August 14, 2004, agree with aircraft measurements. Furthermore, the retrieved total column averages are always underestimated by less than 1%. The results above provide a basis for CO_2 profile retrievals using ground-based observations in the near-infrared region.

1. Introduction

Remote sensing observations improve our understanding of the spatial and temporal distributions of carbon dioxide (CO_2) in the atmosphere. The Total Carbon Column Observing Network (TCCON) is a network of ground-based Fourier transform spectrometers (FTS). An automated solar observatory measures high-quality incoming solar absorption spectra in the near-infrared region ($4000-9000\ cm^{-1}$) (www.tccon.caltech.edu, [1,2]). Each TCCON instrument has a precise solar tracking system that allows the FTS to record direct sunlight. The absorption spectra are measured under clear skies and can be corrected by the recorded DC-signal for partly cloudy skies [3]. There are 20 sites located worldwide, including both operational and future sites. Although unevenly distributed over the world, the TCCON has good latitudinal coverage and the ensemble of sites retrieve the long-term column-averaged abundance of greenhouse gases, such as carbon dioxide (CO_2), methane (CH_4), nitrous oxide (N_2O), and other trace gases (*e.g.* CO) with high accuracy and high precision [2,4–6].

The difference between column-averaged CO_2 (X_{CO_2}) and surface CO_2 can vary from 2 to 10 ppm or even larger depending on the location and the time of the year [7,8]. Higher surface concentrations usually occur at nighttime or in winter due to CO_2 build-up in a shallow planetary boundary layer (PBL), while surface uptake due to plant growth occurs during daytime or in summer. On both diurnal and seasonal time scales, the variations in X_{CO_2} are smaller than surface CO_2 because they are remotely forced by local fluxes through advection. Compared to surface values, the seasonal variation of X_{CO_2} generally has a time lag in phase with less variability due to the time delay caused by vertical mixing. The variations in X_{CO_2} are only partly driven by the local flux. Synoptic-scale activity has a large impact on the variations in X_{CO_2} due to larger-scale eddy fluxes and the meridional gradient in X_{CO_2}. The simulations by Keppel-Aleks et al. [9] illustrate that the sources of X_{CO_2} variations are related to the north-south gradients of X_{CO_2} and the flux on continental scales [9]. In contrast, the variations in PBL CO_2 are directly influenced by local flux [10]. They show that the PBL CO_2 variability is explained by regional surface fluxes related to land

* Corresponding author. Tel.: +1 818 393 5976.
E-mail address: kl@gps.caltech.edu (L. Kuai).

0022-4073/$ - see front matter © 2012 Elsevier Ltd. All rights reserved.
http://dx.doi.org/10.1016/j.jqsrt.2012.04.024

cover and mesoscale circulation across the PBL. In another study, Stephens et al. [11] concludes that most of current models overpredict the annual-mean midday vertical gradients and consequently lead to an overestimated carbon uptake in the northern lands and an underestimated carbon uptake over tropical forests [11]. Isolating the CO_2 dry air mole fraction in the PBL provides higher sensitivity to the surface-atmosphere fluxes since this is the portion of the atmosphere which is most strongly influenced by surface sources and sinks, and this is the layer which will have the largest changes in CO_2 concentrations from surface effects. The surface flux has a direct influence on the diurnal variations of the PBL CO_2. The mesoscale transport would also cause a horizontal difference in the PBL CO_2 concentration. Therefore, the estimates of the PBL CO_2 could provide regional scale constraints on the surface flux [10]. Additionally, multiple pieces of vertical CO_2 concentration information provide important constraints on atmospheric transport uncertainties when inverting these data for flux estimates.

In this paper, we show that high-resolution spectra of atmospheric absorption can provide information about the vertical distribution of CO_2 in addition to the total column abundance. Three scaling factors defined in three bulk atmospheric layers are retrieved to estimate the CO_2 vertical distribution. Other than the accurately retrieved total column abundance, the vertical variation is represented by the partial column averages in the three bulk atmospheric layers.

Major sources of uncertainty in the TCCON retrievals include those from spectroscopic data, measurement noise, instrument line shape function (ILS), temperature, surface pressure and zero-level offset. Significant effort has been undertaken to reduce the instrumental uncertainties of a TCCON experiment [3,12–15]. An overview of these uncertainties for TCCON measurements is discussed in [2,5]. The column measurements are calibrated and their precision is quantified using *in situ* aircraft profiles [5,16].

This study demonstrates the feasibility of retrieving multiple pieces of CO_2 vertical profile information from the high SNR, high spectral resolution atmospheric spectra obtained from TCCON. To ensure an accurate evaluation of the performance of our profile retrieval algorithm, we have limited our analysis to TCCON spectra acquired from the Park Falls, Wisconsin site, which coincides with *in situ* vertical profiles measured from aircraft. This comparison of ground-based and *in situ* data provides critical validation standards for retrievals of CO_2 profile and total column CO_2. This also enables an accurate error assessment. Our study provides a baseline to guide the next generation of remote sensing measurements for profiling the atmospheric CO_2. A more comprehensive evaluation of vertical profile retrievals from multiple TCCON sites for observing dates spanning nearly a decade and sampling a wider range of atmospheric conditions, seasons, and solar zenith angles is under way.

In the followings TCCON and aircraft data, information analysis, and the setup of the vertically constrained retrieval are described in the next section. An illustration of the profile retrievals using both synthetic and real spectra is discussed in Section 3, in which we use three of aircraft profiles, measured at Park Falls [4] on July 12, July 15, and August 14 in 2004, to evaluate the partial column retrievals from coincident TCCON spectra. The conclusions and discussions follow in Section 4.

2. Data and methodology

2.1. TCCON data

The TCCON X_{CO_2} measurements are precise to better than 0.25% [2,5]. With this precision, the monthly averaged column-integrated data are sufficient to reduce the uncertainties in the global surface carbon sources and sinks [17]. The absolute accuracy of the uncalibrated X_{CO_2} measurements from TCCON is $\sim$1% [5]. These measurements have been calibrated to 0.25% accuracy using aircraft profile data that are themselves calibrated to the World Metrological Organization (WMO) scale over nine TCCON sites (Park Falls, Lamont, Darwin, Lauder, Tsukuba, Karlsruhe, Bremen, Bialystok, Orleans) [5,18]. Consequently, they can be used in combination with *in situ* measurements to provide constraints on continental-scale flux estimates [9,19–22].

The TCCON X_{CO_2} measurements are an important validation source for satellite observations, including those from the Orbiting Carbon Observatory (OCO-2) [23], SCanning Imaging Absorption SpectroMeter for Atmospheric CartograpHY (SCIAMACHY) [24], and Greenhouse Gases Observing Satellite (GOSAT) [25–27]. In contrast to these space-based instruments, which measure reflected sunlight in the near infrared region by looking down from space, the retrievals using TCCON spectra have minimal influences from aerosol, uncertainty in airmass, or variation in land surface properties [2] because the TCCON instruments measure direct incoming sunlight from the ground. Thus, TCCON data serve as a transfer standard between satellite observations and *in situ* networks [1,2,5,6,28]. Because of their high quality, TCCON spectra are some of the best data to attempt the challenging profile retrieval.

2.2. Aircraft in situ profiles

The aircraft *in situ* measurements of CO_2 profiles have higher precision ($\sim$0.2 ppm) and higher accuracy ($\sim$0.2 ppm) [5] than the TCCON and spacecraft observations. We consider these measurements to be the best observations of the true state of the atmospheric CO_2 profile. In this study, the remote sensing measurements of CO_2 over Park Falls, Wisconsin on July 12, 15 and August 14, 2004 [4] are compared with the coincident *in situ* measurements during the Intercontinental Chemical Transport Experiment—North America campaign (INTEX—NA) [29]. Highly precise ($\pm$0.25 ppm) CO_2 profiles were obtained from 0.2 to 11.5 km in about a 20 km radius. Due to the altitude floor and ceiling limitations of the aircraft measurements, additional information for surface and stratospheric values of CO_2 are required. The lowest measured value is at $\sim$200 m above the surface, and it is assumed to be the surface value. The profile above the aircraft ceiling

was derived from age of air calculations and *in situ* measurements on high-altitude balloons [5]. An excellent correlation between the integrated aircraft profiles and the FTS retrieved X_{CO_2} was found [4,5,18,29,30]. Calibration using aircraft data reduced the uncertainty in the retrieved X_{CO_2} by TCCON to 0.25% [2,4,5,18,29].

In this work, we also use aircraft measured CO_2 profiles as our standard. In addition to the comparison of X_{CO_2}, we further look at the difference in the partial columns for three scaling layers. The knowledge of the partial columns can improve our understanding of the vertical distribution of total columns in the atmosphere.

2.3. Information analysis

TCCON measurements of direct incoming solar spectra have a high signal-to-noise ratio (SNR) of ~885 on the InGaAs detector and ~500 on the Si diode detector [4]. This is significantly larger than the GOSAT and OCO-2 measurements of the same spectral region (SNR~300). We use the 1.6 μm CO_2 absorption band, which is measured using the InGaAs detector by TCCON with a spectral resolution of 0.02 cm^{-1} (Fig. 1a). This band is also measured by GOSAT and OCO-2 from space. However, the TCCON spectra have a resolution that is ~10 times finer than those of the spacecraft instruments (*e.g.* OCO-2 Fig. 1b).

We applied information analysis to understand how much information can be gained from a retrieval using TCCON-like measurements [31]. The results of the analysis include degrees of freedom (d_S) and information content (H_S). d_S describes how many (which can be fractional) variables can be independently retrieved from the measurements. In our case, for example, d_S is ~3. This means that we can estimate the CO_2 concentrations for at most 3 layers. Even if our forward model has 71 layers, these 71 layers can be roughly divided into 3 groups, and within each group the CO_2 concentrations are highly correlated while the correlation among groups are minimal. H_S is the ratio of the *a posteriori* uncertainty to the *a priori* uncertainty, taken by the logarithm of 2. It thus describes how our knowledge about the measured quantity is improved after making the measurement.

The analysis shows that d_S for signal of the CO_2 from TCCON retrieval is 3.6, 3.8 and 4.3 for solar zenith angle (SZA) 22.5°, 58° and 80°, respectively, assuming that SNR is 885 for TCCON measurements and the *a priori* covariance matrix is diagonal, whose diagonal values is taken $(3\%)^2$ (Table 1). H_S is also listed in Table 1. The instrument noise level has been a key parameter in most retrievals [32]. In our case using TCCON measurements, however, d_S can be as high as 2.7 and 2.8 for SZA equal to 22.5° and 58°, respectively, even for SNR to be as low as 300. A similar calculation for OCO-2 only gives 1.5 d_S because this measurement has lower resolution and lower SNR than TCCON.

Profile information is believed to be imprinted in the absorption line shape through, *e.g.*, pressure broadening. The Jacobian of the absorption spectra of CO_2 ($\mathbf{J}_{CO_2}$)

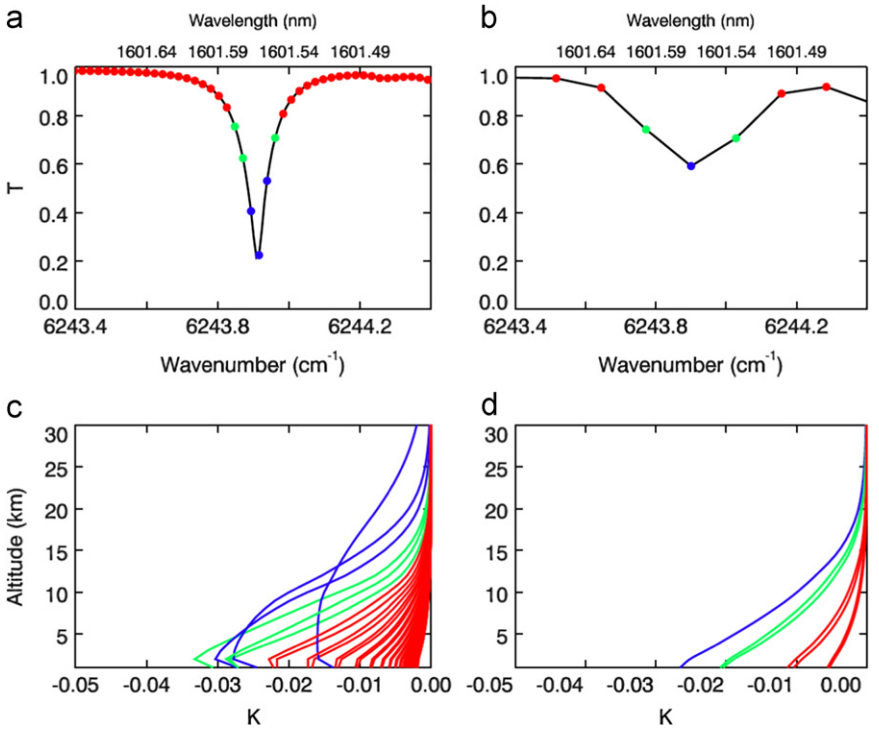

Fig. 1. Simulation of the same absorption line centered at 6243.9 cm^{-1} by (a) TCCON, SZA=22.5° and (b) OCO-2, SZA=17°. The colored dots indicate the channel centers. Their corresponding unitless Jacobian ($\mathbf{J}_{CO_2}=d$[Transmittance]/d[ln(CO_2)]) profiles are plotted in the two bottom panels for (c) TCCON and (d) OCO-2. The weak absorption channels are in red; the intermediate absorption channels are in green; the strong absorption channels are in blue. (For interpretation of the references to color in this figure legend, the reader is referred to the web version of this article).

Table 1
Information analysis for CO_2 retrievals from TCCON and OCO-2 spectra.

	Number of channels	SNR	SZA (°)	Information content: H_S (Bits)	Degree of freedom: d_S
TCCON	10620	885	80	14.4	4.3
TCCON	10620	885	58	12.5	3.8
TCCON	10620	300	58	7.4	2.8
TCCON	10620	885	22.5	11.6	3.6
TCCON	10620	300	22.5	6.8	2.7
OCO-2	1016	300	17	4.23	1.5

concentrations describes the spectral sensitivity to CO_2 changes at different atmospheric levels. The vertical profiles of $\mathbf{J}_{CO_2}$ for TCCON measurements have peaks located at different levels at different frequencies. Fig. 1 shows the CO_2 Jacobian profiles for the frequencies at the same absorption lines but measured by two instruments with different spectral resolutions (TCCON and OCO-2). With its high spectral resolution, the TCCON instrument is able to capture channels with strong absorption that are very close to an absorption line center. Its $\mathbf{J}_{CO_2}$ profiles have broader peaks in the middle and upper troposphere (blue in Fig. 1a and c). Some of the intermediate absorption channels (green) can have stronger peaks than both weak and strong absorption channels which are located in the lower troposphere. The weak absorption channels have the highest sensitivity near the surface. In contrast, the $\mathbf{J}_{CO_2}$ for OCO-2 are all maximized near the surface because its spectral resolution is not sufficient to capture the channels close enough to the line center that could provide complementary information higher up (Fig. 1b and d).

We decide to develop a retrieval algorithm for estimating three partial column averages. The atmosphere will be divided into three bulk layers according to three principles. First, these three layers should represent PBL, lower troposphere and middle-to-upper troposphere. Second, individual d_S for each layer should be approximately equal [33]. Lastly, the pressure weightings (*i.e.* partial air column) contributing to the total air column for these three layers should not differ too much. We arrived at the layer selection by simply determining the lowest layer to be below ~2.5 km for a representation of the PBL (Layer 1). It has ~0.8 d_S and accounts for ~25% of the total air column. Another layer is from 2.5 to 5.5 km (Layer 2), which covers the lower troposphere with ~0.6 d_S; this layer contributes ~25% to the total air column. The third layer is for altitudes above 5.5 km (Layer 3). It has ~1.3 d_S and has the remaining 50% of the total air column. Note that the total air column contribution above the tropopause (~12 km) is negligible. Therefore, Layer 3 can effectively be regarded as a middle-to-upper tropospheric layer. Fig. 2 shows how the three partial columns are distributed.

2.4. Retrievals

The slant column of each absorber is obtained by a nonlinear least-squares spectral fitting routine that uses line-by-line spectroscopic calculations (GFIT, developed at JPL). The radiative transfer model in GFIT computes simulated spectra using 71 vertical levels with 1 km intervals for the input atmospheric state. Details about GFIT are described in [2,4–6,8,30].

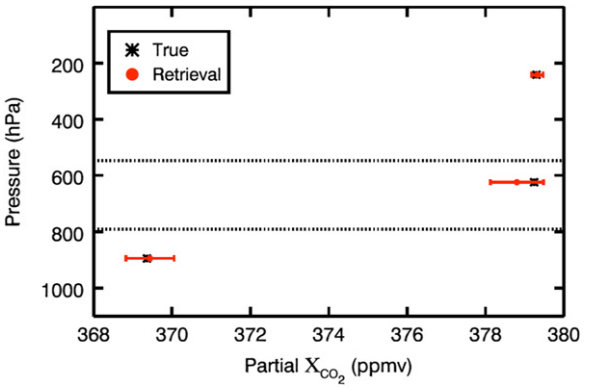

Fig. 2. Comparisons of partial column-averaged CO_2 (pX_{CO_2}) between the synthetic (true) values and the mean (red dot) of pX_{CO_2} from 100 test retrievals. The error bar (units of ppm) is one standard deviation ($1-\sigma$) of the 100 retrieved pX_{CO_2}. Signal-to-noise ratio is 885. Dot lines indicate the top of the three bulk layers defined in the text for profile retrievals. (For interpretation of the references to color in this figure legend, the reader is referred to the web version of this article).

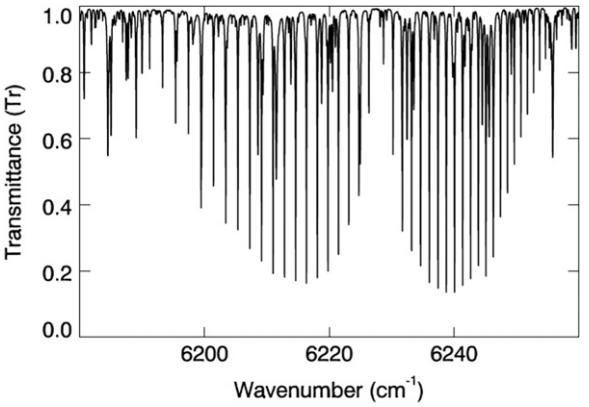

Fig. 3. CO_2 band at 1.6 μm observed on June 17, 2008 by TCCON at Park Falls, Wisconsin with solar zenith angle of 22.5°.

The retrievals in this study fit one of the TCCON-measured CO_2 absorption bands, centered at 6220.00 cm^{-1} with a window width of 80.00 cm^{-1} (Fig. 3), to estimate the atmospheric CO_2 profile. A systematic error of 5 K in temperature profile would cause ~0.35% or ~1 ppm error in X_{CO_2} [6]. This is significantly less sensitive to temperature than the thermal IR band at 15 μm, which has an error of 30 ppm in retrieved CO_2 for an error of 1 K in temperature [34]. To minimize temperature error for CO_2 retrievals, we use assimilated temperature, pressure, and humidity profile for local noon of each day of measurements from the National Centers for Environmental Prediction (NCEP)/ National Center for Atmospheric Research (NCAR) Re-analysis.

The standard TCCON retrieval algorithm uses a "scaling" approach, in which the optimized retrieval is determined by multiplying a predefined vertical profile

with a single scaling factor that is applied to all layers (no adjustments are made to the shape of the profile) [2,5]. The algorithm used in the present study allows for the independent scaling of three separate partial columns while also determining the total column in optimizing the solution [35]. To distinguish the two retrieval algorithms, we call the standard algorithm a "scaling retrieval" and our algorithm a "profile retrieval".

In the scaling retrieval, the retrieved state vector ($\boldsymbol{\gamma}$) includes the eight constant scaling factors for four absorption gases (CO_2, H_2O, HDO, and CH_4) and four instrument parameters (continuum level: '*cl*', continuum title: '*ct*', frequency shift: '*fs*', and zero level offset: '*zo*'):

$$\boldsymbol{\gamma} = \begin{bmatrix} \gamma_{[CO_2]} \\ \gamma_{[H_2O]} \\ \gamma_{[HDO]} \\ \gamma_{[CH_4]} \\ \gamma_{cl} \\ \gamma_{ct} \\ \gamma_{fs} \\ \gamma_{zo} \end{bmatrix} \tag{1}$$

Each element of $\boldsymbol{\gamma}$ is a ratio between the state vector ($\mathbf{x}$) and its *a priori* ($\mathbf{x}_a$). In this work, we improve on the scaling method by replacing $\gamma_{[CO_2]}$ by three values corresponding to the three bulk layers defined in the previous section. The *a priori* CO_2 profiles among the bulk layers can thus be adjusted. For other interfering gases, only single scaling factors are retrieved:

$$\boldsymbol{\gamma} = \begin{bmatrix} \gamma_{1[CO_2]} \\ \gamma_{2[CO_2]} \\ \gamma_{3[CO_2]} \\ \gamma_{[H_2O]} \\ \gamma_{[HDO]} \\ \gamma_{[CH_4]} \\ \gamma_{cl} \\ \gamma_{ct} \\ \gamma_{fs} \\ \gamma_{zo} \end{bmatrix} \tag{2}$$

To obtain the best estimate of $\mathbf{x}$ that minimize the differences between the observed spectral radiances ($\boldsymbol{y}_o$) and the forward model spectral radiances $\boldsymbol{y}_m$, we perform a Bayesian optimization [31] by minimizing the cost function, $\chi(\boldsymbol{\gamma})$:

$$\chi(\boldsymbol{\gamma}) = (\boldsymbol{y}_m - \boldsymbol{y}_o)^T \mathbf{S}_e^{-1} (\boldsymbol{y}_m - \boldsymbol{y}_o) + (\boldsymbol{\gamma} - \boldsymbol{\gamma}_a)^T \mathbf{S}_a^{-1} (\boldsymbol{\gamma} - \boldsymbol{\gamma}_a) \tag{3}$$

By adjusting the *a priori* profile in the three bulk layers, we estimate how the total column-averaged CO_2 is vertically distributed in the atmosphere.

The column amount is usually obtained by integrating the gas concentration profile from z_1 to z_2:

$$C_g = \int_{z_1}^{z_2} f_g(z) \cdot n(z) \cdot dz \tag{4}$$

where C_g is vertical column amount for a target gas 'g' between altitudes z_1 and z_2. When $z_1 = 0$ and $z_2 = \infty$ then C_g is the total column amount. $n(z)$ represents the air number density vertical profile and $f_g(z)$ is dry air gas mole fraction profile.

The ratio of column amount between the target gas and the bulk air will give the column-averaged abundance. The partial column-averaged CO_2 between z_1 and z_2 is simply:

$$pX_{CO_2} = \frac{C_{CO_2}}{C_{air}} = \frac{\int_{z_1}^{z_2} f_{CO_2}(z) \cdot n(z) \cdot dz}{\int_{z_1}^{z_2} f_{air}(z) \cdot n(z) \cdot dz} \tag{5}$$

where f_{CO_2} is dry air CO_2 mole fraction. The total column-averaged CO_2 is

$$X_{CO_2} = \frac{C_{CO_2}}{C_{air}} = \frac{\int_0^{\infty} f_{CO_2}(z) \cdot n(z) \cdot dz}{\int_0^{\infty} f_{air}(z) \cdot n(z) \cdot dz}. \tag{6}$$

3. Profile retrievals

3.1. Synthetic retrievals

We first test the retrieval algorithm using synthetic data before we move forward to more complicated measurements. The advantage of a synthetic study is that we know the "truth" and we can evaluate the precision of the retrievals with different SNR and different *a priori* constraints. The forward model is used both to generate the synthetic spectra and run the retrieval so that errors in spectroscopic data and/or instrument line shapes will not have an effect on the retrieved quantities. This synthetic study also allows us to estimate the errors induced by the uncertainties of the other interference parameters.

A reference transmission spectrum at 6180–6260 cm^{-1} is simulated using the GFIT forward model. Atmospheric profiles including pressure, temperature and humidity are based on NCEP/NCAR Re-analysis at Park Falls on July 12, 2004. One hundred synthetic observational spectra are generated by adding to the reference spectrum some noise of amplitude ε/SNR, where ε is a Gaussian pseudorandom number.

In this paper, we always use one standard deviation ($1-\sigma$) to compute error bars. Assuming there are no uncertainties in the true state of the atmosphere except for the target gas to be retrieved, and that the forward model is perfect, the mean errors (the difference between the retrieved and the true values) in total X_{CO_2} varies from 0.06 to 0.08 ppm, depending on the selection of the layer depths and SNR (885 to 300). Fig. 2 compares the averages of the 100 retrievals of three pX_{CO_2} (red dots) corresponding to the three bulk layers for SNR=885 to the truth (black stars). Their residuals are less than 0.5 ppm. The error bars for the three pX_{CO_2} are no more than 0.7 ppm.

3.2. Realistic retrievals

To compare with the aircraft profile on July 12, 2004, TCCON spectra were selected within a 2-h window centered on the time when the aircraft measurements were taken. The averages of retrievals from these spectra are used to compare with the aircraft measurements.

We propose three tests to study the sensitivity of profile retrieval with respect to *a priori* profiles. In the first test (Test 1), we use an *in situ* aircraft measurement shifted by +1% as the *a priori* profile. In the second test (Test 2), because aircraft CO_2 profiles are not always available at all TCCON sites and in all seasons due to temporal and spatial limitations, we use the *a priori* profiles that have already been used in the scaling retrieval for TCCON measurements [2,36]. In the troposphere (below 10 km), the *a priori* profiles are derived from an empirical model based GLOBALVIEW data [37] while in the stratosphere, an age-dependent CO_2 profile is assumed [38]. In this way, *a priori* profiles for CO_2 at all TCCON sites can be estimated for all seasons. The resultant *a posteriori* CO_2 profiles will be compared to the aircraft measurements. In the third test (Test 3), CO_2 is assumed to be well mixed within each bulk layer defined above. The *a priori* profile in this test is a constant CO_2 of 375 ppm.

In all three tests, the retrieved CO_2 profiles (colored lines in Fig. 4a–c) converged to the aircraft profile ('+' in Fig. 4a–c). Compared with the aircraft measurements, the mean biases in total X_{CO_2} for the three tests are listed along with their precisions in Table 2. In both profile and scaling retrievals, the three tests underestimate the total

Table 2
Bias in total column-averaged CO_2 (X_{CO_2}) from realistic profile retrievals.

Type of retrieval	Bias in total pX_{CO_2} (ppm) (mean $\pm \sigma$)		
	Test 1	Test 2	Test 3
Profile	-0.67 ± 0.25	-0.85 ± 0.24	-0.80 ± 0.24
Scaling	-1.54 ± 0.29	-1.64 ± 0.35	-1.09 ± 0.29

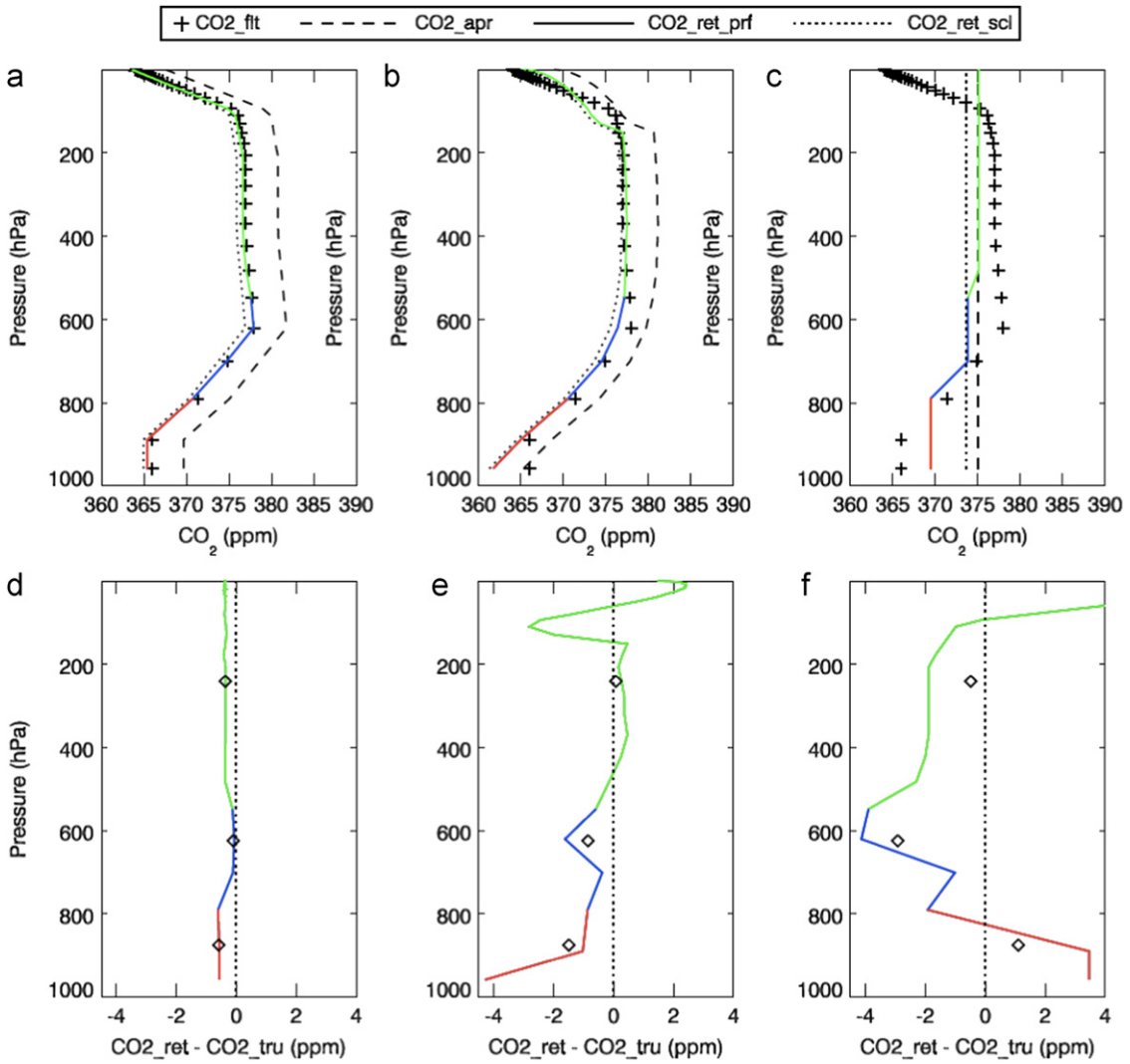

Fig. 4. Examples of profile retrievals from the same spectrum but with three different *a priori* profiles. Solid lines with three different colors in (a)–(c) are retrieved CO_2 derived from the profile retrievals. The differences from the aircraft profile for each case are plotted below them in (d)–(f). The diamonds represent the differences in pX_{CO_2}. This figure demonstrates that the differences in some sublayers can be as large as 4 ppm but the differences in pX_{CO_2} are smaller (< 3 ppm). (For interpretation of the references to color in this figure legend, the reader is referred to the web version of this article.)

X_{CO_2} by 0.67–1.64 ppm, but the profile retrievals always have less bias (<1 ppm) than the scaling retrievals (>1 ppm) for all the three tests. In the profile retrievals, there is a slightly smaller bias in the first test (0.67 ppm) than the other two cases ($\sim$0.8 ppm) likely because the *a priori* profile has the same shape as that measured by the aircraft. However, using other reasonable *a priori* profiles does not lead to a significant. The latter suggests that the retrieval should be robust and is unlikely to be dependent on the profile shape of *a priori*. This agrees with what was found earlier by Wunch et al. [5]. In their scaling retrievals for X_{CO_2}, it is shown that the TCCON *a priori* profiles do not introduce additional bias compared to the results obtained by replacing the *a priori* profile from aircraft measurements with best estimates of the stratospheric profiles.

The vertical resolution in the GFIT model is 1 km from the surface to 70 km with 71 grid points in total. The model layers are divided into three bulk layers mentioned above (surface—2.5 km, 2.5–5.5 km and above 5.5 km). By construction, the shape of the *a priori* profile within a bulk layer remains unchanged during the profile retrieval; it is the scaling factors among the bulk layers that are changed relatively. In the first test, because the shape of the *a priori* profile agrees perfectly with the aircraft profile (Fig. 4a), the difference between the retrieved profile and aircraft profile within the same scaling layer do not vary much with altitude (Fig. 4d colored lines). This is not true in the other two tests where the *a priori* profiles have different shapes from the true profiles (Fig. 4b and c). Although larger differences can occur where the shape of the *a priori* and true profile differs significantly (*e.g.*, Fig. 4e and f), the biases in their partial column averaged CO_2 (diamonds in Fig. 4d, e and f) are much reduced, likely due to the compensation between the sub-layers. Biases and their error bars for the total X_{CO_2} and pX_{CO_2} for multiple retrievals within the 2-h window are listed in Table 3. The error bars in each pX_{CO_2} are no more than 1 ppm. Since the first two layers close to the surface are thinner and therefore less weighted than the third layer, the pX_{CO_2} bias in each layer contribute $\sim$25% to total X_{CO_2} bias according to the pressure weighting function. The third layer accounts for the remaining 50% in the total X_{CO_2} bias. Large uncertainties in the upper atmosphere likely result from the lack of information in the stratosphere.

Here we further discuss the results obtained from Test 2. In particular, the profile retrievals from real measurements using the TCCON *a priori* profiles at Park Falls are compared with the aircraft measurements on July 12 and 15 and August 14 in 2004. The aircraft profiles are integrated vertically to obtain the aircraft total X_{CO_2}. The total X_{CO_2} derived from TCCON and aircraft measurements are plotted in Fig. 5 (diamonds). Table 4 lists the biases and error bars in the retrieved TCCON total X_{CO_2} relative to aircraft total X_{CO_2}. In the 2-h window of the multiple retrievals for approximately the same air mass, the TCCON total X_{CO_2} has a bias of less than 1 ppm for the three-day comparisons and has an average precision of 0.23 ppm. This precision is consistent with the predicted error due to measurement noise of 0.32 ppm [35]. The multiple-day bias of the total X_{CO_2} is -0.3 ppm and the precision is 0.64 ppm. This uncertainty is primarily driven by systematic errors, such as temperature uncertainty, along with the measurement errors. The predicted error from these two terms is 0.78 ppm [35].

Similar error analysis is also applied to the pX_{CO_2} in each bulk layer. The bias and precision for pX_{CO_2} in 2-h window and multiple-day time scale are described in Table 4 and Fig. 5. There are underestimates in the PBL pX_{CO_2} (green dots) and overestimates in the middle-to-upper troposphere (blue dots) and an oscillation in the retrieved profile, which is likely driven by systematic errors in the retrieval. Therefore, there is a relatively large absolute bias in the PBL (Layer 1) and the middle-to-upper troposphere (Layer 3) than in lower troposphere (Layer 2). However, the variability of the bias is larger (about 1 ppm) for the pX_{CO_2} for Layer 2. The oscillation does not affect the estimates of the total X_{CO_2}. With these uncertainties, the estimates of the three pX_{CO_2} are able to capture the vertical gradient of CO_2 in the troposphere. Further error analysis will be done in the future for a more comprehensive study when applying the profile retrieval over multiple sites and over a long-term period.

In the above analysis, we have shown that in addition to the accurate estimates of the total X_{CO_2}, profile retrievals can also provide some vertical information about the CO_2 distribution in the atmosphere in the form of pX_{CO_2}.

Table 3
Same as Table 2, also for partial column-averaged CO_2 (pX_{CO_2}) in the three bulk layers defined in the text. Note that the second column is the same as those for the profile retrievals shown in Table 2.

	Bias in total X_{CO_2}	Bias in pX_{CO_2} (ppm)		
		Layer 1	Layer 2	Layer 3
Test 1	-0.67 ± 0.25	-0.13 ± 0.76	0.25 ± 0.96	-1.30 ± 0.76
Test 2	-0.85 ± 0.24	-1.07 ± 0.76	0.54 ± 0.96	0.87 ± 0.76
Test 3	-0.80 ± 0.24	4.75 ± 0.76	-3.28 ± 0.96	-1.99 ± 0.78

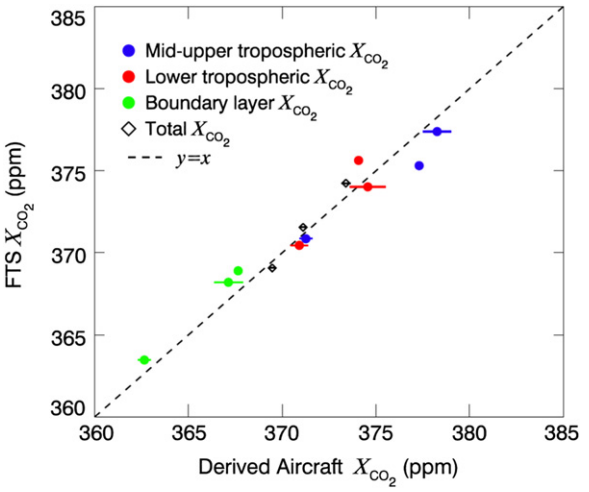

Fig. 5. Calibration curve of total column averages (X_{CO_2}) and three partial column averages (pX_{CO_2}) in the three bulk layers defined in the text. The error bar is the standard deviation ($1-\sigma$) of the retrievals within the 2-h window of aircraft measurements. The pX_{CO_2} in the planetary boundary layer (Layer 1) is underestimated and the pX_{CO_2} in middle-to-upper troposphere (Layer 3) is overestimated.

Table 4
Same as Table 3, for comparisons to the column averaged aircraft data on different dates. TCCON *a priori* profiles (from Test 2, Table 3) are applied to all profile retrievals.

Date in 2004	Bias in total X_{CO_2}	Bias in partial X_{CO_2} (ppm)		
		Layer 1	Layer 2	Layer 3
07/12	-0.85 ± 0.24	-1.07 ± 0.76	0.54 ± 0.96	0.87 ± 0.76
07/15	-0.44 ± 0.19	-1.25 ± 0.11	-1.56 ± 0.21	0.42 ± 0.34
08/14	0.40 ± 0.16	-0.82 ± 0.34	0.46 ± 0.45	1.99 ± 0.21
Mean bias $\pm$ precision	-0.30 ± 0.64	-1.05 ± 0.22	-0.19 ± 1.19	1.09 ± 0.81

4. Conclusions

TCCON provides long-term ground-based observations to help understand the CO_2 variations at different timescales and at different latitudes. In addition to the column measurements, information on the vertical distribution of CO_2 can be obtained from these observations. Our retrieval simulations have confirmed their potential for retrieving the CO_2 profile. The realistic profile retrievals from TCCON spectra are compared to *in situ* CO_2 profiles measured by aircraft. The comparison between the retrieved X_{CO_2} and the integration of the aircraft CO_2 profiles show an underestimate from both scaling and profile retrievals. This agrees with the conclusion from the previous work on the calibration of TCCON data against aircraft measurements. The ratio of the X_{CO_2} determined from FTS scaling retrievals to that from integrated aircraft profiles gives a correction factor of 0.991 ± 0.002 (mean $\pm$ standard deviation of the ratios of FTS to aircraft X_{CO_2}) at Park Falls [4,5]. However, Wunch et al. [5] also retrieved CO_2 from the another band at 6339 cm^{-1}, and computed the average of two retrievals before they are scaled by the retrieved O_2 to a mean value of 0.2095 in order to get the dry air column-averaged mole fractions [4,5,8,30]. Here the results we presented are the retrievals from one of two windows mentioned above, which is centered at 6220 cm^{-1}. The column-averaged dry-air mole fraction is derived using the pressure weighting function which was introduced in Connor et al. [39], instead of being scaled by simultaneously retrieved O_2. The scaling by retrieved O_2 reduces systematic errors that are common to both CO_2 and O_2 (such as pointing errors and ILS errors), but does not necessarily reduce the overall bias.

In this paper, we have expanded the standard scaling retrieval of X_{CO_2} to three partial columns and demonstrated that profile retrievals are possible on high-resolution spectra. The profile retrievals generate consistent results with the scaling retrievals and add extra information about the vertical CO_2 distribution. The retrieved pX_{CO_2} in the free troposphere can be more readily compared with satellite retrievals from thermal infrared spectra such as AIRS and TES that are more sensitive to the mid-troposphere. Long-term profile data can be useful to address variability at different time scales and at different altitudes. The direct use of profile data for inverse modeling can provide better constraints on the CO_2 sources and sinks on regional scales and also on the atmospheric transport uncertainties.

For a future comprehensive study, the following tests can help us to improve the retrieved results. Using the synthetic retrieval simulations we can test the sensitivity of retrieved partial columns to ± 5 K temperature bias and $\pm 10\%$ specific humidity bias. We can estimate the sensitivity to different seasons or latitudes, when the water column, temperature profile, and solar zenith angle will all be different.

Acknowledgments

This research is supported in part by the Orbiting Carbon Observatory 2 (OCO-2) project, a NASA Earth System Science Pathfinder (ESSP) mission and Project JPL.1382974 to the California Institute of Technology. Support for TCCON and operations at Park Falls Wisconsin are provided by a grant from NASA to the California Institute of Technology (NNX11AG01G). We would like to thank Gretchen Keppel Aleks, Mimi Gerstell, Vijay Natraj, Sally Newman, Jack Margolis, Xi Zhang, King-Fai Li, and Michael Line for useful discussions and comments on the paper. Special thanks are given to G. Toon and P. Wennberg for making available their code and data, and for valuable discussions.

References

[1] Wunch D, Wennberg PO, Toon GC, Keppel-Aleks G, Yavin YG. Emissions of greenhouse gases from a North American megacity. Geophys Res Lett 2009;36:L15810, http://dx.doi.org/10.1029/2009gl039825.
[2] Wunch D, Toon GC, Blavier JFL, Washenfelder RA, Notholt J, Connor BJ, et al. The Total Carbon Column Observing Network (TCCON). Philos Trans R Soc a-Math Phys Eng Sci 2011;369:2087–112.
[3] Keppel-Aleks G, Toon GC, Wennberg PO, Deutscher NM. Reducing the impact of source brightness fluctuations on spectra obtained by Fourier-transform spectrometry. Appl Opt 2007;46:4774–9.
[4] Washenfelder RA, Toon GC, Blavier JF, Yang Z, Allen NT, Wennberg PO, et al. Carbon dioxide column abundances at the Wisconsin Tall Tower site. J Geophys Res-Atmos 2006;111:D22305, http://dx.doi.org/10.1029/2006jd007154.
[5] Wunch D, Toon GC, Wennberg PO, Wofsy SC, Stephens BB, Fischer ML, et al. Calibration of the Total Carbon Column Observing Network using aircraft profile data. Atmos Meas Tech 2010;3:1351–62.
[6] Yang ZH, Toon GC, Margolis JS, Wennberg PO. Atmospheric CO_2 retrieved from ground-based near IR solar spectra. Geophys Res Lett 2002;29:1339.
[7] Olsen SC, Randerson JT. Differences between surface and column atmospheric CO_2 and implications for carbon cycle research. J Geophys Res-Atmos 2004;109 [Art. no.-D02301].
[8] Geibel MC, Gerbig C, Feist DG. A new fully automated FTIR system for total column measurements of greenhouse gases. Atmos Meas Tech 2010;3:1363–75.

[9] Keppel-Aleks G, Wennberg PO, Schneider T. Sources of variations in total column carbon dioxide. Atmos Chem Phys 2011;11:3581–93.
[10] Sarrat C, Noilhan J, Lacarrere P, Donier S, Lac C, Calvet JC, et al. Atmospheric CO_2 modeling at the regional scale: application to the CarboEurope Regional Experiment. J Geophys Res-Atmos 2007:112.
[11] Stephens BB, Gurney KR, Tans PP, Sweeney C, Peters W, Bruhwiler L, et al. Weak northern and strong tropical land carbon uptake from vertical profiles of atmospheric CO(2). Science 2007;316: 1732–5.
[12] Abrams MC, Toon GC, Schindler RA. Practical example of the correction of Fourier-transform spectra for detector nonlinearity. Appl Opt 1994;33:6307–14.
[13] Gisi M, Hase F, Dohe S, Blumenstock T. Camtracker: a new camera controlled high precision solar tracker system for FTIR-spectrometers. Atmos Meas Tech 2011;4:47–54.
[14] Hase F, Blumenstock T, Paton-Walsh C. Analysis of the instrumental line shape of high-resolution Fourier transform IR spectrometers with gas cell measurements and new retrieval software. Appl Opt 1999;38:3417–22.
[15] Messerschmidt J, Macatangay R, Notholt J, Petri C, Warneke T, Weinzierl C. Side by side measurements of CO_2 by ground-based Fourier transform spectrometry (FTS). Tellus B 2010;62:749–58.
[16] Messerschmidt J, Geibel MC, Blumenstock T, Chen H, Deutscher NM, Engel A, et al. Calibration of TCCON column-averaged CO(2): the first aircraft campaign over European TCCON sites. Atmos Chem Phys 2011;11:10765–77.
[17] Rayner PJ, O'Brien DM. The utility of remotely sensed CO_2 concentration data in surface source inversions. Geophys Res Lett 2001;28:175–8.
[18] Messerschmidt J, Geibel MC, Blumenstock T, Chen H, Deutscher NM, Engel A, et al. Calibration of TCCON column-averaged CO_2: the first aircraft campaign over European TCCON sites. Atmos Chem Phys Discuss 2011;11:14541–82.
[19] Gurney KR, Chen YH, Maki T, Kawa SR, Andrews A, Zhu ZX. Sensitivity of atmospheric CO_2 inversions to seasonal and interannual variations in fossil fuel emissions. J Geophys Res-Atmos 2005:110.
[20] Gurney KR, Law RM, Denning AS, Rayner PJ, Baker D, Bousquet P, et al. Towards robust regional estimates of CO_2 sources and sinks using atmospheric transport models. Nature 2002;415:626–30.
[21] Chevallier F, Deutscher NM, Conway TJ, Ciais P, Ciattaglia L, Dohe S, et al. Global CO(2) fluxes inferred from surface air-sample measurements and from TCCON retrievals of the CO(2) total column. Geophys Res Lett 2011:38.
[22] Chevallier F. Impact of correlated observation errors on inverted CO(2) surface fluxes from OCO measurements. Geophys Res Lett 2007:34.
[23] Crisp D, Atlas RM, Breon FM, Brown LR, Burrows JP, Ciais P, et al. The Orbiting Carbon Observatory (OCO) mission. Adv Space Res 2004;34:700–9.
[24] Bosch H, Toon GC, Sen B, Washenfelder RA, Wennberg PO, Buchwitz M, et al. Space-based near-infrared CO_2 measurements: testing the Orbiting Carbon Observatory retrieval algorithm and validation concept using SCIAMACHY observations over Park Falls, Wisconsin. J Geophys Res-Atmos 2006;111:D23302, http://dx.doi.org/10.1029/2006jd007080.
[25] Sato M, Tahara S, Usami M. FIP's environmentally conscious solutions and GOSAT. Fujitsu Sci Tech J 2009;45:134–40.
[26] Yokomizo M. Greenhouse gases Observing SATellite (GOSAT) Ground Systems. Fujitsu Sci Tech J 2008;44:410− +.
[27] Yokota T, Yoshida Y, Eguchi N, Ota Y, Tanaka T, Watanabe H, et al. Global Concentrations of CO_2 and CH_4 retrieved from GOSAT: first preliminary results. Sola 2009;5:160–3.
[28] Reuter M, Bovensmann H, Buchwitz M, Burrows JP, Connor BJ, Deutscher NM, et al. Retrieval of atmospheric CO_2 with enhanced accuracy and precision from SCIAMACHY: validation with FTS measurements and comparison with model results. J Geophys Res-Atmos 2011;116:D04301, http://dx.doi.org/10.1029/2010JD015047.
[29] Singh HB, Brune WH, Crawford JH, Jacob DJ, Russell PB. Overview of the summer 2004 intercontinental chemical transport experiment—North America (INTEX-A). J Geophys Res-Atmos 2006;111(D24s01). http://dx.doi.org/10.1029/2006jd007905.
[30] Deutscher NM, Griffith DWT, Bryant GW, Wennberg PO, Toon GC, Washenfelder RA, et al. Total column CO_2 measurements at Darwin, Australia—site description and calibration against *in situ* aircraft profiles. Atmos Meas Tech 2010;3:947–58.
[31] Rodgers CD. In: Inverse methods for atmospheric sounding: theory and practice. London: World Scientific; 2000.
[32] O'Dell CW, Day JO, Pollock R, Bruegge CJ, O'Brien DM, Castano R, et al. Preflight radiometric calibration of the orbiting carbon observatory. IEEE Trans Geosci Remote Sensing 2011;49:2438–47.
[33] Natraj V, Liu X, Kulawik S, Chance K, Chatfield R, Edwards DP, et al. Multi-spectral sensitivity studies for the retrieval of tropospheric and lowermost tropospheric ozone from simulated clear-sky GEO-CAPE measurements. Atmos Environ 2011;45:7151–65.
[34] Kulawik SS, Jones DBA, Nassar R, Irion FW, Worden JR, Bowman KW, et al. Characterization of Tropospheric Emission Spectrometer (TES) CO(2) for carbon cycle science. Atmos Chem Phys 2010;10: 5601–23.
[35] Kuai L, Worden J, Kulawik S, Bowman K, Biraud4 S, Natraj V, et al. Profiling tropospheric CO_2 using the Aura TES and TCCON instruments. Atmos Meas Tech Discuss, submitted for publication.
[36] Toon GC. The JPL MkIV interferometer. Opt Photonics News 1991;2: 19–21.
[37] GLOBALVIEW-CO_2: Cooperative Atmospheric Data Integration Project—carbon dioxide, CD-ROM, NOAA ESRL, Boulder, Colorado, also available on Internet via anonymous FTP to fpt.cmd1.noaa.gov, las access: July 2009, Path: ccg/co2/GLOBALVIEW; 2008.
[38] Andrews AE, Boering KA, Daube BC, Wofsy SC, Loewenstein M, Jost H, et al. Mean ages of stratospheric air derived from *in situ* observations of CO_2, CH_4, and N_2O. J Geophys Res-Atmos 2001;106: 32295–314.
[39] Connor BJ, Boesch H, Toon G, Sen B, Miller C, Crisp D. Orbiting carbon observatory: inverse method and prospective error analysis. J Geophys Res Atmos 2008;113:D05305, http://dx.doi.org/10.1029/2006jd008336.